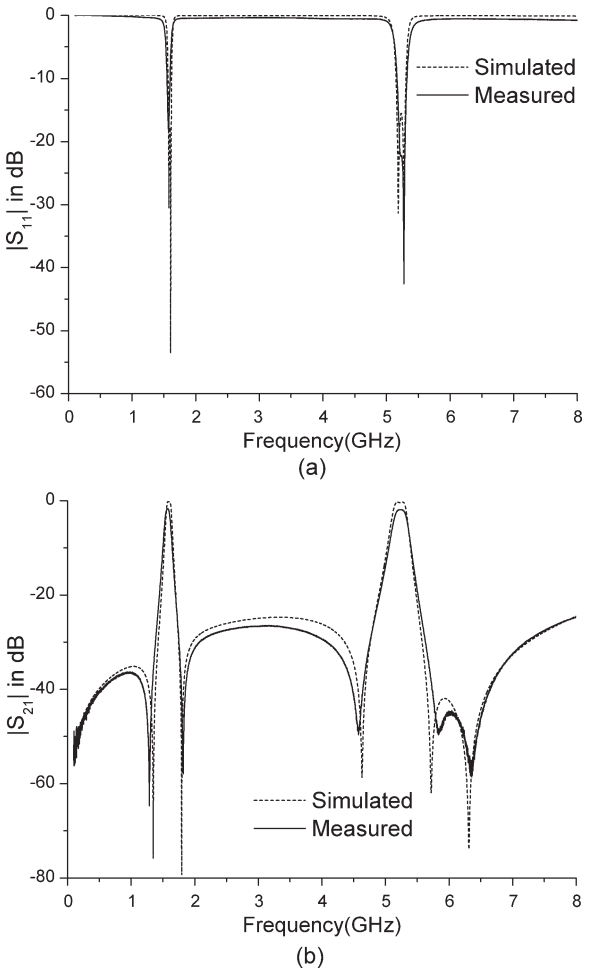

Figure 7 Simulated and measured frequency responses of the dual-band microstrip BPF

transmission zeros T_{z1} and T_{z3} are separately created near the lower cut-off frequency of the first passband and the second passband due to the main path signal counteraction [8], and the location of the transmission zeros T_{z2} and T_{z4} near the upper cut-off frequencies are mainly controlled by the short-circuited stubs [11]. To deepen the upper-stopband, the transmission zero T_{z5} is created in the upper-stopband owing to source-load coupling. As l_4 increases, the transmission zero T_{z5} moves near the upper cut-off frequencie. Considering the out-band performance, we choose $l_4 = 8.65$ mm.

After studying the characteristic of the compact and high selectivity dual-band dual-mode microstrip BPF with source-load coupling, a filter is fabricated on the RT/Duroid 5880 substrate through the standard printed circuit board (PCB) fabrication process, and its photograph is shown in Figure 6. The filtering performance is measured by Agilent network analyzer N5230A. The simulated and measured frequency responses shown in Figure 7 agree with each other. It can be seen that the insertion losses are 1.62 and 1.42 dB, and S_{11} is 18 and 24.2 dB at 1.575 and 5.2 GHz, respectively. The 3-dB bandwidths are 0.1 GHz from 1.55 to 1.65 and 0.24 GHz from 5.1 to 5.34 GHz. Therefore, the relative 3-dB bandwidths are 6.3 and 4.6% at 1.58 and 5.2 GHz, respectively. Five transmission zeros (T_{z1}, T_{z2}, T_{z3}, T_{z4}, and T_{z5}) are located at 1.23, 1.84, 4.62, 5.81, and 6.38 GHz to result in sharp skirt, with an attenuation level of less than -27.2dB. The upper-stopband in experiment is extended up to 8 GHz with an insertion loss better than -23.2 dB.

4. CONCLUSIONS

In this letter, a compact and high selectivity dual-band dual-mode microstrip BPF with the source-load coupling is proposed using one single short-circuited stub loaded SIR. The resonator can generate one odd mode resonant frequencies and one even mode ones in each band, and the even mode ones can be only determined by the short-circuited stub at the central. The filter utilizes the resonator's fundamental odd and even mode resonant frequencies and second harmonic resonant frequencies to generate two passbands. Five transmission zeros are created near the passband edges and in the upper-stopband to improve the selectivity. The measured result agrees with the electromagnetics (EM) simulation.

REFERENCES

1. L.-C. Tsai and C.-W. Hsue, Dual-band bandpass filters using equal-length coupled-serial-shunted lines and Z-transform technique, IEEE Trans Microwave Theory Tech 52 (2004), 1111–1117.
2. Y.P. Zhang and M. Sun, Dual-band microstrip bandpass filter using stepped-impedance resonators with new coupling schemes, IEEE Trans Microwave Theory Tech 54 (2006), 3779–3885.
3. S. Sun and L. Zhu, Compact dual-band microstrip bandpass filter without external feed, IEEE Microwave Wirel Compon Lett 15 (2005), 644–646.
4. J.-T. Kuo, T.-H. Yeh, and C.-C. Yeh, Design of microstrip bandpass filter with a dual-passband response, IEEE Trans Microwave Theory Tech 53 (2005), 1331–1337.
5. M.-H. Weng, H.-W. Wu, and Y.-K. Su, Compact and low loss dual-band bandpass filter using pseudo-interdigital stepped impedance resonators for WLANs, IEEE Microwave Wirel Compon Lett 17 (2007), 187–189.
6. S. Gao, Z.-Y. Xiao, and W.-F. Chen, Dual-band bandpass filter with source-load coupling, Electron Lett 45 (2009), 894–895.
7. C.-Y. Chen and C.-Y. Hsu, A simple and effective method for microstrip dual-band filters design, IEEE Microwave Wirel Compon Lett 16 (2006), 246–248.
8. M. Zhou, X. Tang, and F. Xiao, Compact dual band transversal bandpass filter with multiple transmission zeros and controllable bandwidths, IEEE Microwave Wirel Compon Lett19(2009).
9. M.-L. Chuang, M.-T. Wu, and S.-M. Tsai, Dual-band filter design using L-shaped stepped impedance resonators, IET Microwave Antennas Propag 4 (2009), 855–862.
10. M.-L. Chuang, Dual-band microstrip coupled filters with hybrid coupling paths, IET Microwave Antennas Propag 4 (2010), 947–954.
11. S.W. Wong and L. Zhu, Quadruple-mode UWB bandpass filter with improved out-of-band rejection, IEEE Microwave Wirel Compon Lett 19 (2009), 152–154.

SMALL-SIZE MULTIBAND PLANAR ANTENNA FOR LTE700/2300/2500 OPERATION IN THE TABLET COMPUTER

Kin-Lu Wong,[1] Chao-An Lyu,[1] and Liang-Che Chou[2]
[1] Department of Electrical Engineering, National Sun Yat-Sen University, Kaohsiung 804, Taiwan; Corresponding author: wongkl@ema.ee.nsysu.edu.tw
[2] Department of High Frequency Business, Yageo Corporation Nantze Branch, Kaohsiung 811, Taiwan

Received 18 March 2011

ABSTRACT: *A small-size multiband planar antenna can be obtained using a long parasitic shorted strip and a monopole feed encircled by the same. Such a configuration can lead to a small antenna size for multiband operation, and a promising design with a small size of 12 ×*

35 mm^2 for covering three-band LTE700/2300/2500 operation (704–787/2300–2400/2500–2690 MHz bands) in the tablet computer is presented. The antenna is easy to fabricate on one surface of an FR4 substrate and is composed of an inverted-L strip as the monopole feed and a long parasitic shorted strip encircling the inverted-L monopole. The long shorted strip is parasitically excited to generate a 0.25-wavelength resonant mode at about 750 MHz to cover the LTE700 operation, while the inverted-L monopole generates a 0.25-wavelength resonant mode at about 2.5 GHz to cover the LTE2300/2500 operation. Details of the proposed antenna are described. Radiation characteristics of the antenna and its body specific absorption rate results for tablet computer applications are also presented. © 2011 Wiley Periodicals, Inc.
Microwave Opt Technol Lett 54:81–86, 2012; View this article online at wileyonlinelibrary.com. DOI 10.1002/mop.26507

Key words: *mobile antennas; internal tablet computer antennas; multiband antennas; LTE antennas; small antennas*

1. INTRODUCTION

The long-term evolution (LTE) operation is becoming demanded for modern mobile devices such as the smartphones, laptop computers, and tablet computers. The LTE operation can provide much higher communication data rate than the wireless wide area network (WWAN) operation and mainly include three operation bands of the LTE700 (704–787 MHz), LTE2300 (2300–2400 MHz), and LTE2500 (2500–2690 MHz). Some promising WWAN/LTE internal antennas for mobile devices have also been reported [1–11]. These antennas can cover all the operating bands of the WWAN and LTE operations and are attractive to be used in the mobile devices as the main internal antenna for voice and data communications. However, it is noted that the LTE is best suited for the multiple-input multiple-output (MIMO; Refs. 12–14) operation. For the LTE MIMO operation, a second LTE antenna will be required to be embedded in the mobile devices to combine with the main antenna (WWAN/LTE antenna) to form a 1 × 2 LTE array to achieve much higher communication data rates. For this application, a three-band LTE700/2300/2500 antenna with a size much smaller than the main antenna (WWAN/LTE antenna) will be very attractive for the LTE MIMO operation in the mobile devices. In the published papers for the present, however, there are very few promising LTE antennas that occupy a small size and are capable of covering all the LTE700/2300/2500 bands for mobile device applications.

In this article, we present a small-size planar printed LTE antenna which is easy to fabricate and requires a small size of 12 × 35 mm^2 for covering the three-band LTE700/2300/2500 operation in the tablet computer. The proposed antenna applies the design technique of using a long parasitic shorted strip and a monopole feed encircled by the same to achieve multiband operation with a small antenna size. The long parasitic shorted strip contributes to its fundamental (0.25-wavelength) resonant mode at about 750 MHz to cover the LTE700 operation. The monopole feed in this study is an inverted-L strip which contributes to its fundamental (0.25-wavelength) resonant mode at about 2.5 GHz to cover the LTE2300/2500 operation. In addition to the small size for multiband operation obtained for the antenna, it is easy to adjust the resonant modes contributed, respectively, by the long parasitic shorted strip and the inverted-L monopole encircled by the same. Detailed operating principle of the proposed antenna is described. Radiation characteristics of the antenna and its body specific absorption rate (SAR; Ref. 15–17) results for 1-g tissue in the bottom face and edge (landscape and portrait) conditions [15] for tablet computer applications are also analyzed.

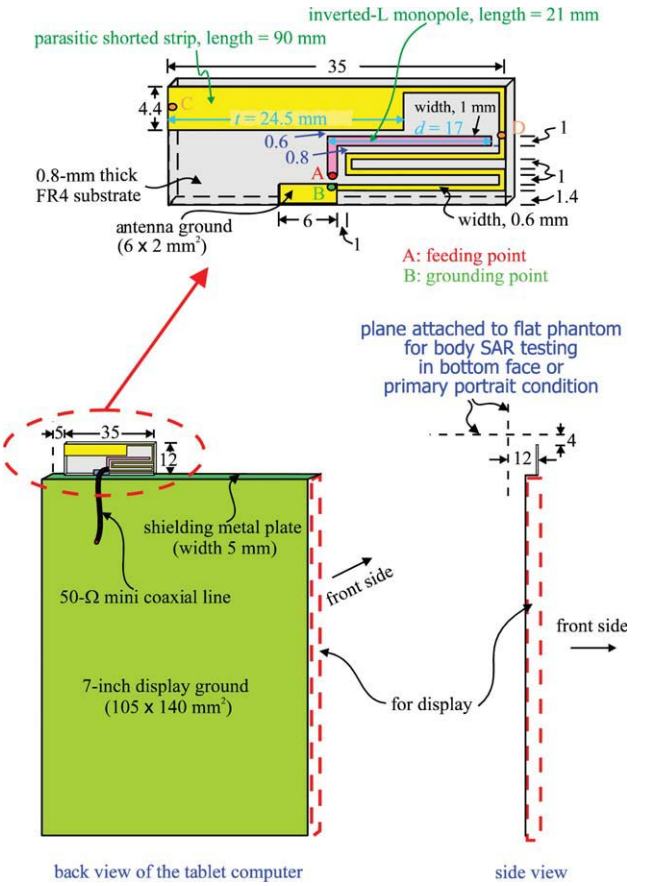

Figure 1 Geometry of the proposed internal LTE700/2300/2500 antenna for tablet computer application. [Color figure can be viewed in the online issue, which is available at wileyonlinelibrary.com]

2. DESIGN CONSIDERATIONS OF PROPOSED LTE ANTENNA

Figure 1 shows the geometry of the proposed small-size multiband planar printed antenna for the LTE700/2300/2500 operation in the tablet computer. The antenna is printed on one surface of an FR4 substrate of size 12 × 35 mm^2, relative permittivity 4.4, and loss tangent 0.02, and it is mounted along the front edge of the metal wall at one edge of display ground. The metal wall has a size of 5 × 105 mm^2, which is connected to one edge of the display ground of dimensions 105 × 140 mm^2. In the study, both the metal wall and the display ground are made by a 0.2-mm-thick copper plate, and the display ground supports a 7-in. display; that is, a 7-in. tablet computer is considered in this study, which is commercially available for the present.

The antenna comprises a long parasitic shorted strip and an inverted-L monopole encircled by the same. The antenna is fed using a 50-Ω minicoaxial line (see the photo in Fig. 2 for the

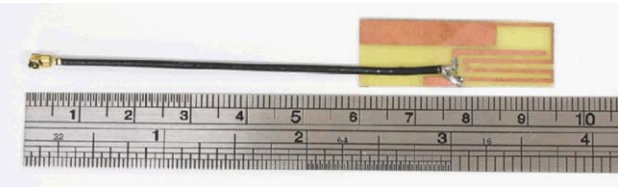

Figure 2 Photo of the fabricated antenna. [Color figure can be viewed in the online issue, which is available at wileyonlinelibrary.com]

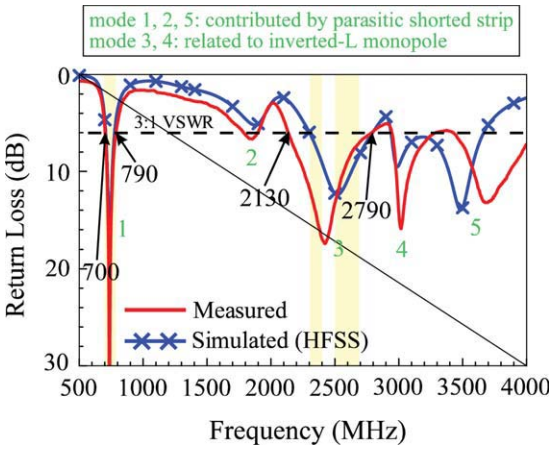

Figure 3 Measured and simulated return loss for the proposed antenna. [Color figure can be viewed in the online issue, which is available at wileyonlinelibrary.com]

fabricated antenna connected to a 50-Ω minicoaxial line), whose central conductor is connected to the feeding point (point A) of the inverted-L monopole, and outer grounding sheath is connected to the grounding point (point B) at the antenna ground (size 6 × 2 mm^2) which is further connected to the metal wall. Note that the antenna is also mounted close to one corner of the metal wall with a distance of 5 mm. This can allow other possible internal antennas to be accommodated along the metal wall.

The parasitic shorted strip has a length of about 90 mm (close to 0.25-wavelength at 750 MHz), with its front end short-circuited to the antenna ground. The parasitic shorted strip can generate a 0.25-wavelength resonant mode at about 750 MHz to cover the LTE700 operation. Its widened open end of width 4.4 mm and length (t) 24.5 mm can enhance the bandwidth and decrease the resonant frequency of the excited resonant mode. The inverted-L monopole has a length of 21 mm (close to 0.25-wavelength at 2.5 GHz) and contributes to a 0.25-wavelength resonant mode for the LTE2300/2500 operation. With the parasitic shorted strip encircling the inverted-L monopole, a compact

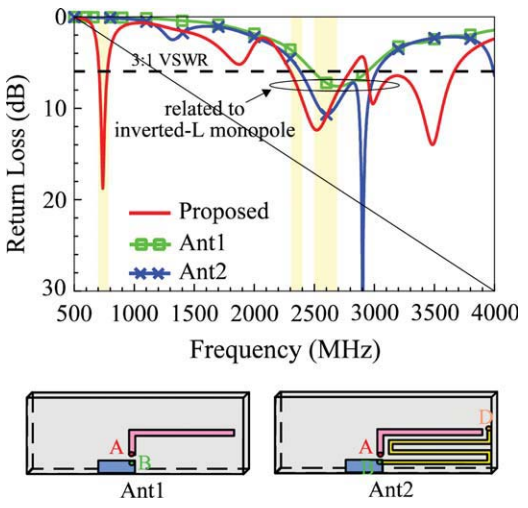

Figure 4 Simulated return loss for the proposed antenna, the case with the inverted-L monopole only (Ant1), and the case with the inverted-L monopole and a portion of the shorted strip (Ant2). [Color figure can be viewed in the online issue, which is available at wileyonlinelibrary.com]

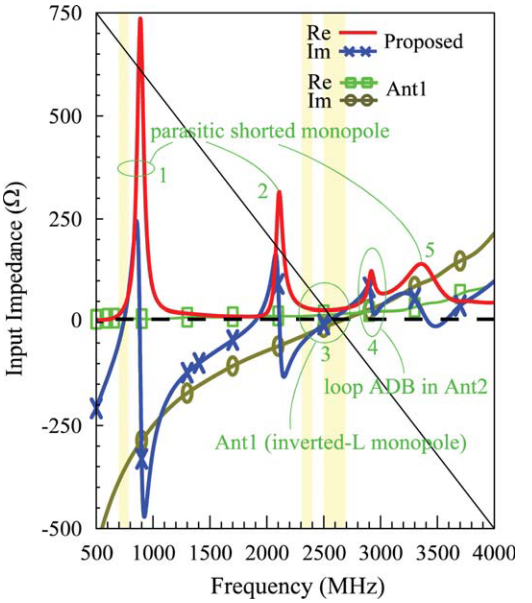

Figure 5 Simulated input impedance for the proposed antenna and the case with the inverted-L monopole only (Ant1). [Color figure can be viewed in the online issue, which is available at wileyonlinelibrary.com]

configuration for the antenna can be obtained. Further, the desired antenna's lower band for the LTE700 operation and upper band for the LTE2300/2500 operation can be easily controlled, respectively, by the parasitic shorted strip and the inverted-L monopole. In addition, a portion of the parasitic shorted strip can combine with the inverted-L monopole to provide an additional loop resonant path (loop ADB, see Fig. 1 and Ant2 in Fig. 4), which contributes to additional resonant mode for the antenna. Higher-order resonant modes of the parasitic shorted strip are also generated which further increases the bandwidths of the antenna. Detailed operating principle and the excited resonant modes of the antenna will be discussed in Section 3.

3. RESULTS OF PROPOSED ANTENNA

The proposed antenna was fabricated (see Fig. 2, a photo of the fabricated antenna) and tested in this study. Figure 3 shows the measured and simulated return loss of the antenna tested with

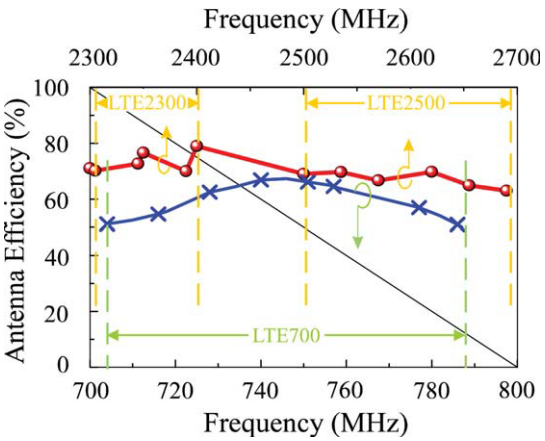

Figure 6 Measured antenna efficiency (mismatching loss included) for the proposed antenna. [Color figure can be viewed in the online issue, which is available at wileyonlinelibrary.com]

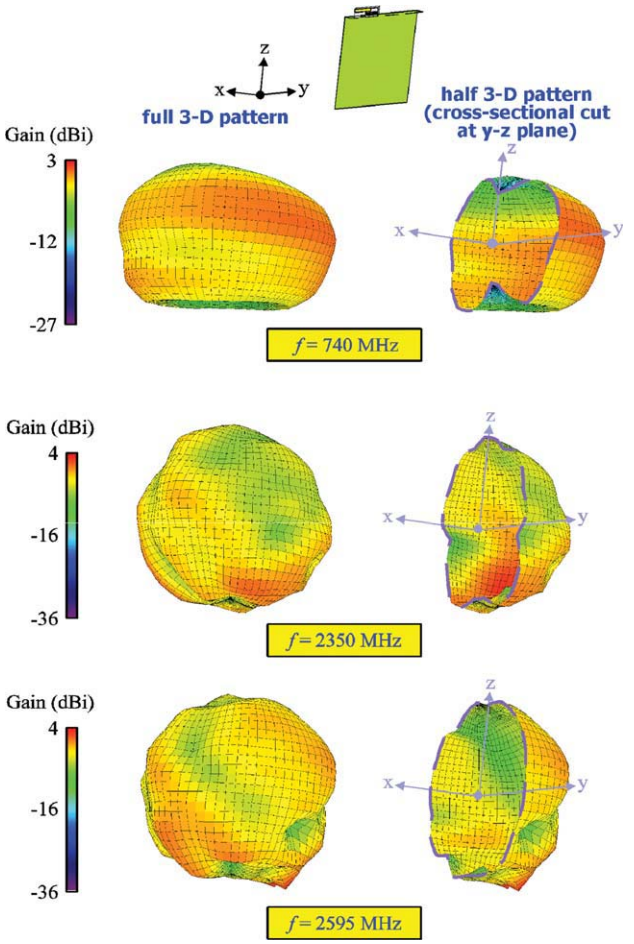

Figure 7 Measured three-dimensional total-power radiation patterns for the proposed antenna. [Color figure can be viewed in the online issue, which is available at wileyonlinelibrary.com]

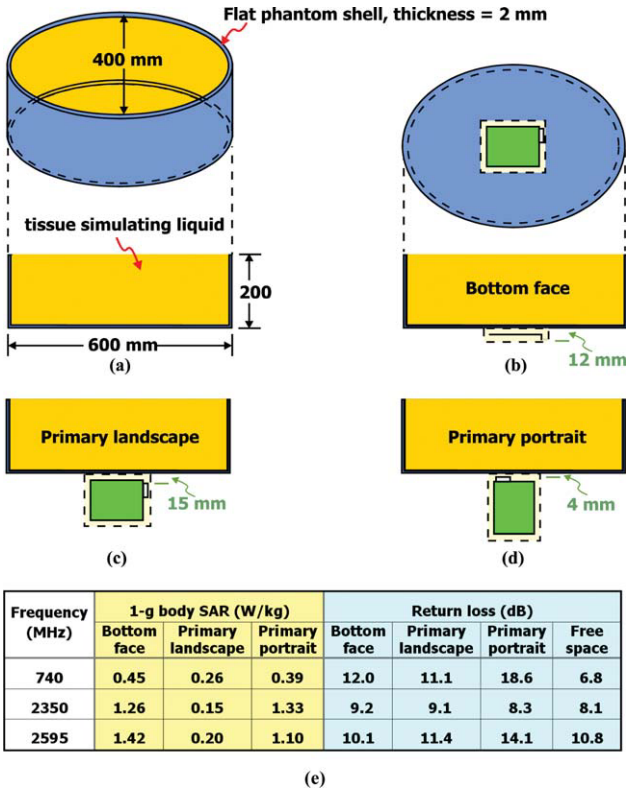

Frequency (MHz)	1-g body SAR (W/kg)			Return loss (dB)			
	Bottom face	Primary landscape	Primary portrait	Bottom face	Primary landscape	Primary portrait	Free space
740	0.45	0.26	0.39	12.0	11.1	18.6	6.8
2350	1.26	0.15	1.33	9.2	9.1	8.3	8.1
2595	1.42	0.20	1.10	10.1	11.4	14.1	10.8

(e)

Figure 8 Body SAR simulation models. (a) Flat phantom simulating the body tissue. (b) Bottom face SAR model. (c) Primary landscape SAR model. (d) Primary portrait SAR model. (e) Body SAR values for 1-g body tissue. [Color figure can be viewed in the online issue, which is available at wileyonlinelibrary.com]

the display ground and metal wall. Simulated return loss is obtained using the simulation software HFSS version 12 [18]. Agreement between the simulation and measurement is seen. On the basis of the 3:1 VSWR or 6-dB return loss, a widely used design specification for the internal WWAN and LTE mobile device antennas, the obtained bandwidths cover the LTE700 operation in the 704–787 MHz and the LTE2300/2500 operation in the 2300–2400/2500–2690 MHz. Note that there are five resonant modes excited below 4 GHz for the antenna. Among them, Mode 1 at about 750 MHz, Mode 2 at about 2 GHz, and Mode 5 at about 3.5 GHz are mainly contributed by the parasitic shorted strip, with Mode 1 the 0.25-wavelength mode of the parasitic shorted strip and Modes 2 and 5 the higher-order resonant modes of the parasitic shorted strip. Mode 3 at about 2.4 GHz and Mode 4 at about 3 GHz are related to the inverted-L monopole, with Mode 3 the 0.25-wavelength mode of the inverted-L monopole and Mode 4 contributed by the loop path ADB seen in Ant2 in Figure 4.

Figure 4 shows the simulated return loss for the proposed antenna, the case with the inverted-L monopole only (Ant1), and the case with the inverted-L monopole and a portion of the shorted strip (Ant2). The corresponding simulated input impedance for the proposed antenna and Ant1 is shown in Figure 5. For Ant1, a resonant mode excited at about 2.5 GHz is shown in Figure 4, which coincides with the condition of a resonance (zero reactance) occurred at about 2.5 GHz as shown in Figure 5 for both the proposed antenna and Ant1. When the parasitic shorted strip is added to form the proposed antenna, additional resonant modes at about 0.75, 2.0, 3.0, and 3.5 GHz are generated (note that the one at 3.0 GHz is contributed by the loop path ADB), and the impedance matching of the resonant mode at about 2.5 GHz contributed by Ant1 is also improved to cover the LTE2300/2500 operation. The resonant mode at about 0.75 GHz covers the LTE700 operation, while the resonant mode at about 2.5 GHz covers the LTE2300/2500 operation. In addition, it is interesting to note that the resonant mode at about 3.5 GHz is promising to cover the WiMAX operation in the 3.5 GHz band [19–21].

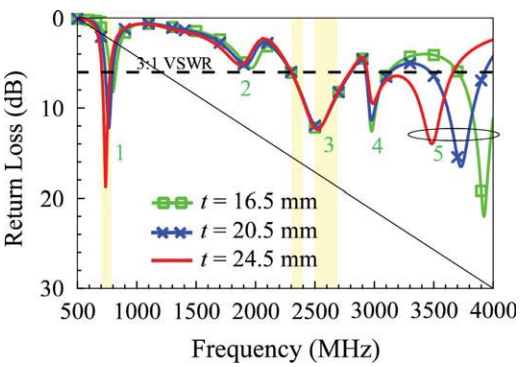

Figure 9 Simulated return loss as a function of the open-end section length t of the parasitic shorted strip. Other parameters are the same as in Figure 1. [Color figure can be viewed in the online issue, which is available at wileyonlinelibrary.com]

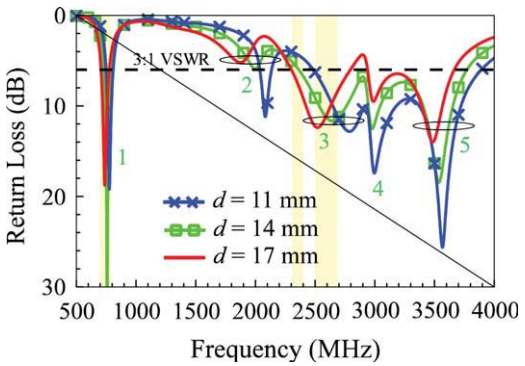

Figure 10 Simulated return loss as a function of the open-end section length d of the inverted-L monopole. Other parameters are the same as in Figure 1. [Color figure can be viewed in the online issue, which is available at wileyonlinelibrary.com]

Radiation characteristics of the fabricated antenna with the display ground and metal wall were also measured in a far-field anechoic chamber. Figure 6 shows the measured antenna efficiency which includes the mismatching loss. Over the LTE700 and LTE2300/2500 bands, the efficiency is varied, respectively, in about 50–76% and 62–80%. The measured antenna efficiency is all better than about 50% and good for practical applications. Figure 7 plots the measured three-dimensional total-power radiation patterns for the antenna. Note that the display ground is in the y–z plane in the figure. At 740 MHz, dipole-like radiation pattern is seen, which is similar to that observed at about 900 MHz for many reported internal WWAN mobile handset antennas [22–26]. This behavior indicates that although the display ground supporting a 7-in. display in this study is as large as 105 $\times$ 140 mm^2, which is about or larger than twice that (about 100 $\times$ 60 mm^2) of the system ground plane of conventional smartphones, the radiation patterns of the LTE internal antennas are still dominated by the system ground plane of the mobile device. At 2350 and 2595 MHz, the radiation patterns are also similar to those seen at about 2 GHz for the reported internal WWAN mobile handset antennas [22–26]. The obtained results suggest that the radiation patterns of the internal LTE antenna in the tablet computer with a 7-in. display show similar behavior as those observed for the internal WWAN mobile handset antennas.

Figure 8 shows the body SAR simulation models based on the simulation software SEMCAD X version 14 [27] and the obtained 1-g SAR values. The flat phantom used to simulate the body tissue is shown in Figure 8(a). Inside the flat phantom is the tissue simulating liquid [28]. The body SAR testing conditions include the bottom face condition shown in Figure 8(b) and two edge conditions (primary landscape and primary portrait) shown in Figure 8(c) and (d). The obtained 1-g SAR values are listed in the table in Figure 8(e). Note that the antenna in the two other edge conditions of secondary landscape and secondary portrait has a large distance of larger than 50 mm to the flat phantom and will have a very small SAR values (usually less than 0.1 W/kg for 1-g tissue). Hence, the two other edge conditions are not tested in the study. The return loss given in the table indicates the impedance matching level of the antenna at each testing frequency. The input power for the SAR testing is 0.125 W (21 dBm) for the LTE operation. The obtained SAR values for 1-g tissue are all less than 1.6 W/kg, making the proposed antenna promising for practical tablet computer applications.

4. PARAMETRIC STUDY

A parametric study of some design parameters of the antenna is also conducted. Figure 9 shows the simulated return loss as a function of the open-end section length t of the parasitic shorted strip. Results for the length t varied from 16.5 to 24.5 mm are presented. No effects on Mode 3 which is mainly contributed by the inverted-L monopole are seen, while there are some variations seen for the other four modes (Modes 1, 2, 4, and 5), especially Modes 1, 2, and 5 which are mainly controlled by the parasitic shorted strip. For Mode 4, as discussed in Figures 4 and 5, it is controlled by the loop path ADB and hence in part affected by the parasitic shorted strip.

Figure 10 shows the simulated return loss as a function of the open-end section length d of the inverted-L monopole. Large effects on Modes 3 and 4 are seen. However, significant effects on Modes 1, 2, and 5 are also observed. This is probably because the variation in the length d also affects the excitation of the parasitic shorted strip, thus resulting in the excitation of Modes 1, 2, and 5. From the results, the desired operating bands for the antenna to cover the LTE700 and LTE2300/2500 operation can be effectively adjusted by tuning the length t in the parasitic shorted strip and the length d in the inverted-L monopole, respectively.

5. CONCLUSIONS

A small-size planar LTE700/2300/2500 antenna suitable for tablet computer applications has been proposed. The antenna has also been fabricated and tested. The antenna has a planar structure and is easy to fabricate by printing on an FR4 substrate of size 12 $\times$ 35 mm^2. The two desired operating bands for covering the LTE700 (704–787 MHz) and LTE2300/2500 (2300–2690 MHz) are easily, respectively, controlled by the parasitic shorted strip and the inverted-L monopole of the antenna. Good radiation characteristics for frequencies over the three LTE bands have been observed. The antenna is also promising to meet the 1-g SAR limit of 1.6 W/kg required for practical applications in the tablet computer.

REFERENCES

1. T.W. Kang, K.L. Wong, L.C. Chou, and M.R. Hsu, Coupled-fed shorted monopole with a radiating feed structure for eight-band LTE/WWAN operation in the laptop computer, IEEE Trans Antennas Propag 59 (2011), 674–679.
2. F.H. Chu and K.L. Wong, Simple planar printed strip monopole with a closely-coupled parasitic shorted strip for eight-band LTE/GSM/UMTS mobile phone, IEEE Trans Antennas Propag 58 (2010), 3426–3431.
3. S.C. Chen and K.L. Wong, Small-size 11-band LTE/WWAN/WLAN internal mobile phone antenna, Microwave Opt Technol Lett 52 (2010), 2603–2608.
4. K.L. Wong and C.T. Lee, Wideband surface-mount chip antenna for eight-band LTE/WWAN slim mobile phone application, Microwave Opt Technol Lett 52 (2010), 2554–2560.
5. K.L. Wong, W.Y. Chen, C.Y. Wu, and W.Y. Li, Small-size internal eight-band LTE/WWAN mobile phone antenna with internal distributed LC matching circuit, Microwave Opt Technol Lett 52 (2010), 2244–2250.
6. K.L. Wong, M.F. Tu, C.Y. Wu, and W.Y. Li, Small-size coupled-fed printed PIFA for internal eight-band LTE/GSM/UMTS mobile phone antenna, Microwave Opt Technol Lett 52 (2010), 2123–2128.
7. S.C. Chen and K.L. Wong, Bandwidth enhancement of coupled-fed on-board printed PIFA using bypass radiating strip for eight-band LTE/GSM/UMTS slim mobile phone, Microwave Opt Technol Lett 52 (2010), 2059–2065.

8. K.L. Wong and W.Y. Chen, Small-size printed loop-type antenna integrated with two stacked coupled-fed shorted strip monopoles for eight-band LTE/GSM/UMTS operation in the mobile phone, Microwave Opt Technol Lett 52 (2010), 1471–1476.
9. C.T. Lee and K.L. Wong, Planar monopole with a coupling feed and an inductive shorting strip for LTE/GSM/UMTS operation in the mobile phone, IEEE Trans Antennas Propag 58 (2010), 2479–2483.
10. C.W. Chiu, C.H. Chang, and Y.J. Chi, A compact folded loop antenna for LTE/GSM band mobile phone applications, In: International conference on electromagnetics in advanced applications (ICEAA), 2010, pp. 382–385.
11. T.W. Kang and K.L. Wong, Internal printed loop/monopole combo antenna for LTE/GSM/UMTS operation in the laptop computer, Microwave Opt Technol Lett 52 (2010), 1673–1678.
12. G. Park, M. Kim, T. Yang, J. Byun, and A.S. Kim, The compact quad-band mobile handset antenna for the LTE700 MIMO application, In: IEEE AP-S int symp., Charleston, SC, 2009.
13. Q. Rao and D. Wang, Compact low coupling dual-antennas for MIMO applications, In: IEEE AP-S int. symp., Charleston, SC, 2009.
14. M.S. Han and J. Choi, Multiband MIMO antenna with a band stop filter for high isolation characteristics, In: IEEE AP-S int symp., Charleston, SC, 2009.
15. Federal Communications Commission, Office of Engineering and Technology, Mobile and Portable Device RF Exposure Equipment Authorization Procedures, OET/Lab Knowledge Database publication number 447498 item 7, December 13, 2007.
16. American National Standards Institute (ANSI), Safety levels with respect to human exposure to radio-frequency electromagnetic field, 3 kHz to 300 GHz, ANSI/IEEE standard C95.1, April 1999.
17. IEC 62209–1, Human exposure to radio frequency fields from hand-held and body-mounted wireless communication devices—Human models, instrumentation, and procedures—Part 1: Procedure to determine the specific absorption rate (SAR) for hand-held devices used in close proximity to the ear (frequency range of 300 MHz to 3 GHz), February 2005.
18. ANSYS HFSS, http://www.ansys.com/products/hf/hfss/.
19. C.T. Lee and K.L. Wong, Uniplanar printed coupled-fed PIFA with a band-notching slit for WLAN/WiMAX operation in the laptop computer, IEEE Trans Antennas Propag 57 (2009), 1252–1258.
20. C.I. Lin, K.L. Wong, and S.H. Yeh, Wideband EMC chip antenna for WLAN/WiMAX operation in the sliding mobile phone, Microwave Opt Technol Lett 48 (2006), 1362–1366.
21. P.Y. Lai and K.L. Wong, Capacitively-fed hybrid monopole/slot antenna for 2.5/3.5/5.5 GHz WiMAX operation in the mobile phone, Microwave Opt Technol Lett 50 (2008), 2689–2694.
22. K.L. Wong, W.Y. Chen, and T.W. Kang, On-board printed coupled-fed loop antenna in close proximity to the surrounding ground plane for penta-band WWAN mobile phone, IEEE Trans Antennas Propag 59 (2011), 751–757.
23. K.L. Wong and S.C. Chen, Printed single-strip monopole using a chip inductor for penta-band WWAN operation in the mobile phone, IEEE Trans Antennas Propag 58 (2010), 1011–1014.
24. Y.W. Chi and K.L. Wong, Quarter-wavelength printed loop antenna with an internal printed matching circuit for GSM/DCS/PCS/UMTS operation in the mobile phone, IEEE Trans Antennas Propag 57 (2009), 2541–2547.
25. C.H. Chang and K.L. Wong, Printed λ/8-PIFA for penta-band WWAN operation in the mobile phone, IEEE Trans Antennas Propag 57 (2009), 1373–1381.
26. C.I. Lin and K.L. Wong, Printed monopole slot antenna for internal multiband mobile phone antenna, IEEE Trans Antennas Propag 55 (2007), 3690–3697.
27. SPEAG SEMCAD, Schmid & Partner Engineering AG, http://www.semcad.com.
28. Tissue Simulating Liquid for SAR Measurement, NTT Advanced Technology Corporation http://www.ntt-at.com/products_e/sar/index.html.

A COMPACT OPEN-ENDED SLOT ANTENNA DESIGN FOR ULTRAWIDEBAND APPLICATIONS

Chow-Yen-Desmond Sim,[1] Chih-Wei Tseng,[1] and Wei-Chung Weng[2]
[1] Department of Electrical Engineering, Feng Chia University, Taichung 40724, Taiwan, Republic of China
[2] Department of Electrical Engineering, National Chi Nan University, Nantou 54561, Taiwan, Republic of China; Corresponding author: wcweng@ncnu.edu.tw

Received 23 March 2011

ABSTRACT: *A compact size slot antenna designed for ultrawideband (UWB) applications is proposed. The slot embedded into the antenna was comprised an open-ended hemicircular slot and a narrow rectangular slot. To achieve good impedance matching within the desired band of interest, the 50 Ω microstrip feed-line is loaded with an elliptical slot, while an extended substrate was protruded above the upper edge of the antenna. The experimental results such as return losses, radiation patterns, and gain properties are studied, and good characteristics are demonstrated. Typical frequency domain responses are also measured to ensure that the proposed antenna can provide stable signal transmission within the UWB spectrum.* © 2011 Wiley Periodicals, Inc. Microwave Opt Technol Lett 54:86–91, 2012; View this article online at wileyonlinelibrary.com. DOI 10.1002/mop.26514

Key words: *ultrawideband; slot antenna; open-ended*

1. INTRODUCTION

The ultrawideband (UWB) systems for short distance mobile communication applications are widely studied after the release of UWB spectrum in 2002 from the Federal Communication Commission that covers 3.1–10.6 GHz. As the antenna is one of the most important elements in a UWB communication system, a UWB antenna that exhibits a 7.5 GHz bandwidth, with an omnidirectional radiation pattern and a stable transmission characteristic, is desirable for the commercial domain. A variety of UWB antennas have been extensively studied recently in the open-literature [1–8]. To achieve the desirable antenna performances such as near omnidirectional pattern, steady gain, and good transmission characteristics, while exhibiting the advantages such as low-cost and ease in fabrication, the planar monopole antenna designs are commonly proposed. However, conventional planar UWB antennas may exhibit a large aperture size (larger than $0.6\lambda_o$), which results in difficulty to integrate with mobile communication devices with compact sizes. Thus, planar UWB antennas with close-end slot designs are proposed [9–14], so that wideband characteristics can be achieved while enable a size reduction in antenna size. However, these designs [9–14] have demonstrated unstable antenna's gain due to smaller radiating area of the antennas. To overcome the disadvantages mentioned above, planar UWB antennas with open-ended slots are proposed [15–21]. By simply loading one or more open-ended slots (slits) into the ground plane (can also be considered as the radiating element in this case), the desirable UWB spectrum can be achieved with compact size as small as $0.28\lambda \times 0.145\lambda$ [15], $0.27\lambda \times 0.16\lambda$ [16], and $0.3\lambda \times 0.135\lambda$ (Ref. 21; refer to 3.0 GHz). From the aforementioned references in the open-literature, such design method with electrical dimension of around $0.25\lambda \times 0.15\lambda$ is rarely reported.

Therefore, in this article, a compact size ($0.25\lambda \times 0.15\lambda$) UWB antenna with 10 dB bandwidth operating from 3.09 GHz up to more than 11.0 GHz is proposed. Besides exhibiting a